WIDEBAND CIRCUIT MODELLING OF WAVEGUIDE DISCONTINUITIES BY FD-TD METHODS

Franco Moglie, Tullio Rozzi, Pio Marcozzi
Dipartimento di Elettronica ed Automatica, University of Ancona, Italy
Marco Politi
Alcatel Telettra, Vimercate Milano, Italy

ABSTRACT

FD-TD methods offer, in principle, promise of great flexibility for application to waveguide discontinuities of any kind. The problem of appropriate termination in the guide enviroment has recently been addressed. Main remaining disadvantages are the volume of computation involved, lack of analytical insight and inability, so far, to produce wideband equivalent circuits, which are prerequisites to effective CAD and synthesis. With a view to remedying these shortcomings, we discuss the extraction from the FD-TD analysis of wideband equivalent circuits. Two significant examples are considered: the inductive post and the 90° H-plane corner, including a modified form of the same. The circuits thus obtained are subsequently employed in the CAD problem of matching over the full waveguide band the modified corner by means of two inductive screws. Theoretical and experimental results are in excellent agreement yielding a reflection <-12 dB over the band and showing the effectiveness of the approach.

I. INTRODUCTION

The flexibility offered by direct integration of Maxwell's equations in the time domain (FD-TD) is now well appreciated. Although its introduction dates back to 1966 [1] its application to transmission line problems has only relatively slowly followed the introduction of an effective termination condition for quasi-plane waves [2], such as stripline and microstrip. In a classical waveguide, where the field differs substantially from the quasi-TEM situation, application of the above condition gives inaccurate results. For a homogeneous guide, one has to adopt instead termination conditions that simulate in the time-domain the loading of the accessible modes at either side of the discontinuity by the proper characteristic impedance. Also important for an effective convergence of the solution is the inclusion of the appropriate edge conditions to be satisfied by metal corners [3,4] in the FD-TD process. Once attention is paid to the above points, FD-TD results for waveguide discontinuities can be as accurate as any obtained by analytical methods. Still, the advantage of flexibility of the method is counterbalanced by two drawbacks; one is constituted by the heavy computational means required. Much more essential, however, seems the lack of analytical insight and of resulting wideband equivalent circuits. In principle, however, there is no reason why FD-TD models should not be endowed with all the analytical features of frequency-domain solutions. With a view to remedying said shortcomings, we address the problem of extraction of equivalent circuits of the canonical Foster form from the FD-TD analysis of lossless discontinuities in homogeneous waveguide. This purpose requires, in particular, that the time-domain excitation be chosen in such a way as to yield information over a wide enough frequency range. This aim is achieved, for instance, by employing a Gaussian type distribution centred at midband and of width comparable to the full waveguide band. In the following, we demonstrate the method by application to two examples: modelling of the inductive post and the characterization and matching of the 90° H-plane corner, including an undercut version of the same. The former problem has been solved analytically in [5], whereas a narrow band approximate representation of the corner can be found in [6]. Although various solutions of corner matching problem are possible, for of ease of mechanical construction and of precision at millimetre wave frequencies, we restrict attention to the configuration of figure 1. Here two screws are symmetrically placed on the guide at either side of the corner. By either numerical minimization over the band or, better, by exploiting an impedance inverter prototype at midband, we derive a matched configuration whose reflection is less than -12 dB over the wide waveguide band. This configuration was built and tested, showing excellent agreement between design and experiment.

II. EQUIVALENT CIRCUIT EXTRACTION OF THE ISOLATED INDUCTIVE POST

Details of the FD-TD analysis of cascaded inductive posts can be found in [4]. In order to extract a two-port equivalent circuit of the individual post (one accessible mode), we assume the symmetric lumped T-configuration shown in figure 2. Figures 3 and figure 4 compare typical FD-TD Z-parameters with those obtained in [5]. Their agreement over the significant range of geometrical parameters is so close that the results of the two approaches can be considered as indistinguishable.

III. CIRCUIT MODEL OF THE 90° H-PLANE CORNER

Having tested the new approach on a previously well characterized discontinuity, we now turn to the modelling of the

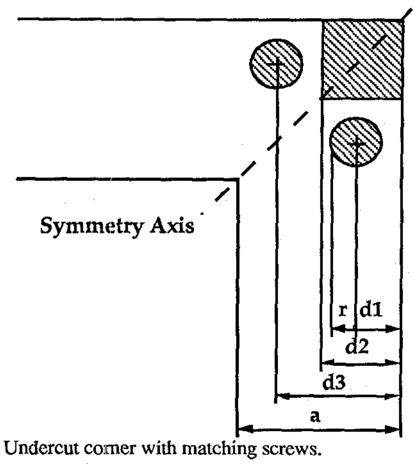

Figure 1. Undercut corner with matching screws.

OF2

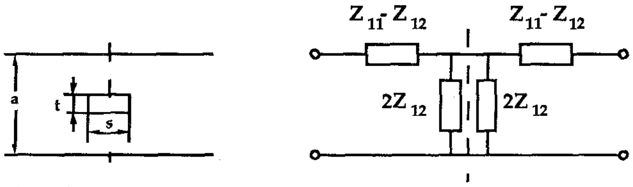

Figure 2. a) top view of the inductive post b) two-port equivalent network.

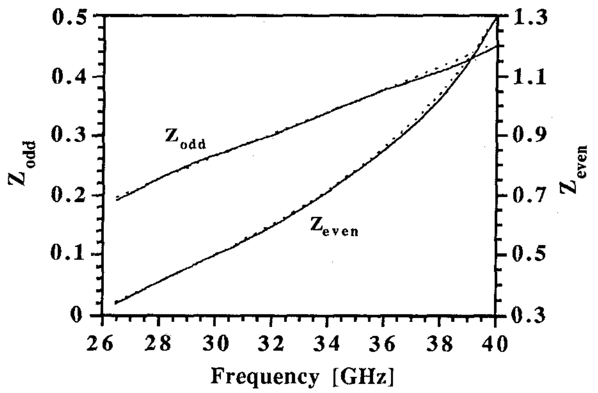

Figure 3. FD-TD (continuous line) and [5] (dashed line) Z-parameters for waveguide inductive post. Post dimensions are: a=7.112 mm, b=3.556 mm, t=0.15 mm and s=2.10 mm.

90° H-plane corner, for which only the approximate, narrow band network model of [6] seems to be available. This is reported in figure 5, while the resulting admittances are plotted versus normalized frequency in figure 6. We now consider the corner undercut as in figure 1. This was preferred to the mitred configuration for ease of fabrication and because it lends itself to matching by inductive screws as reported in the next section. Figure 7 shows a comparison of the scattering parameters of the undercut corner produced by FD-TD field analysis with experimental data.

IV. Wide Band Matching of the 90° H-Plane Corner

Although the undercut corner shows somewhat better reflection properties than the original corner, these were still deemed insufficient for applications. The complementary nature of the power storage mechanism of the undercut corner and that of the screw discontinuity, however, suggests compensating the corner by means of two symmetrically placed identical screws. The band of interest is 36÷40 GHz. We optimized the structure by the equivalent circuit of the post and 90° H-plane corner and using FD-TD for fine tuning. The optimized circuit was built and tested at K_A-band, with dimensions reported in table 1. In figure 8 are reported numerical results obtained with a standard discretization (λ/30), those of a finer discretization (λ/60) in order to account more accurately for the round edges of the screw, as well as experimental results. The good convergence of the method and its accuracy, as compared to experiment, are therefore shown.

V. Spatial Distribution of Energy of 90° H-Plane Corner

In order to account for the spatial distribution of electrical and

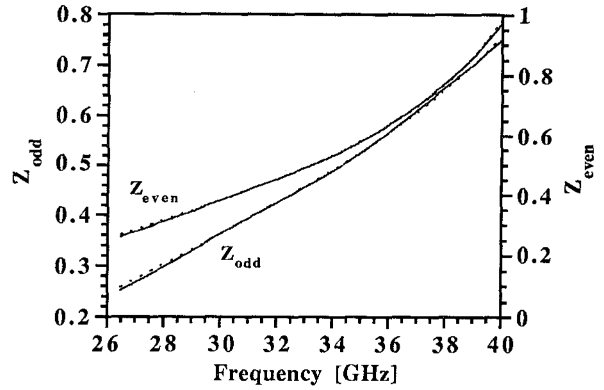

Figure 4. FD-TD (continuous line) and [5] (dashed line) Z-parameters for waveguide inductive post. Post dimensions are: a=7.112 mm, b=3.556 mm, t=0.15 mm and s=6.00 mm.

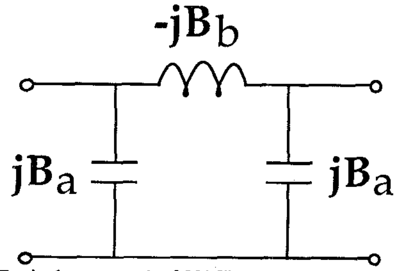

Figure 5. Equivalent network of 90° H-plane waveguide corner.

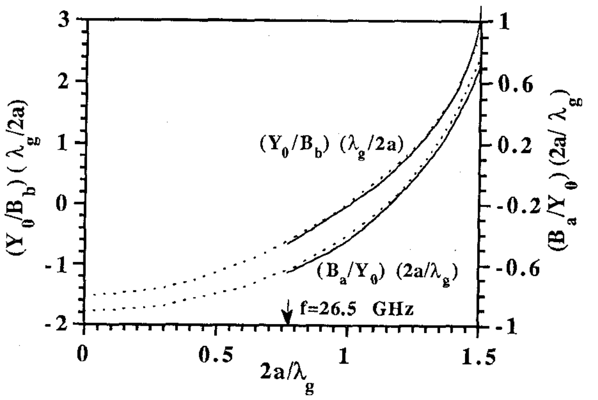

Figure 6. FD-TD (continuous line) and [6] (dashed line) Y-parameters of 90° H-plane waveguide corner.

magnetic energy, the 90° H-plane corner was excited using a sinusoidal pulse at different frequencies. After the time behaviour reached the steady condition we recovered the distribution of the energy by computing

$$\frac{\varepsilon_0|E|^2}{2} \quad \text{and} \quad \frac{\mu_0|H|^2}{2}$$

for the electrical and magnetic energy respectively. In the figures the excitation comes from the left. All results are obtained exciting the waveguide with an electric filed whose

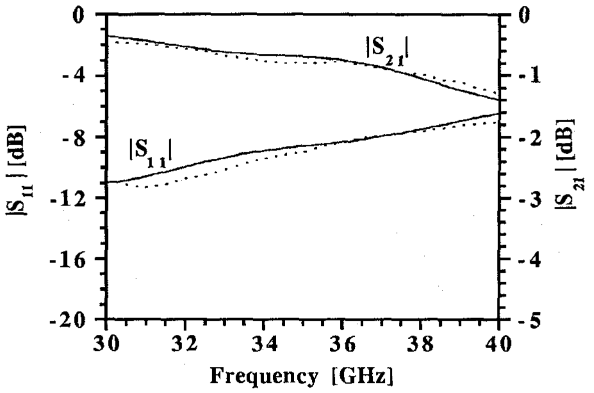

Figure 7. FD-TD (continuous line) and measured (dashed line) S-parameters of 90° H-plane waveguide undercut corner.

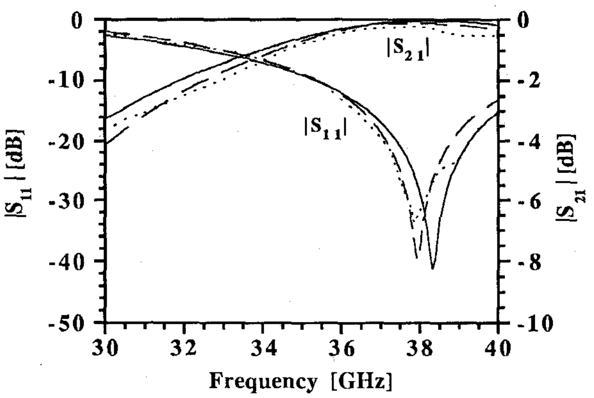

Figure 8. Comparison between FD-TD (continuous line and long dashed line for less accurate simulation) and measured (short dashed line) of 90° H-plane waveguide undercut corner matched by screws.

maximum value is 100 V/m. Figure 9 reports the electrical energy distribution at a frequency of 33 GHz, while in figure 10 is reported the magnetic energy distribution for the same frequency. It seems from two figures that there is more energy in the electric field even though the only modes excited by the discontinuity are TE_{n0} modes. It is straightforward to show that the two figures reflect the physical behaviour if we take into account that return loss value of the corner is 7 dB at 33 GHz: taking TE_{10} incidence and -7 dB TE_{10} reflected wave the distribution of energy is as shown in the figures (clearly this is

Element	Length [mm]
a	7.112
b	3.556
r	1.000
d1	1.967
d2	3.480
d3	5.447

Table 1. Dimensions of the optimized circuit. Actual fabrication sets the following constraints: r=1 mm, d2<a/2, d1+r < a/2, d1-r > 0.5 mm, d3+r <a and d3-r > a/2 + 0.5 mm.

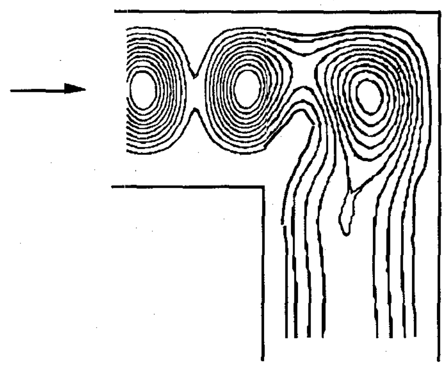

Figure 9. Electric energy distribution for f=33 Ghz. $E_{max}=9.68\cdot10^{-8}$ J/m^3.

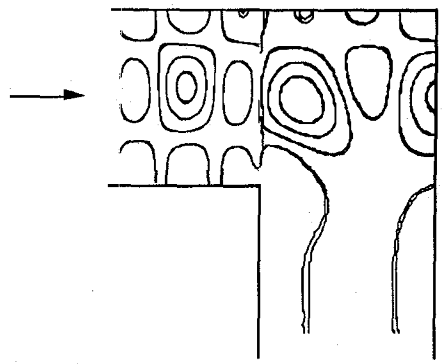

Figure 10. Magnetic energy distribution for f=33 Ghz. $E_{max}=4.32\cdot10^{-8}$ J/m^3.

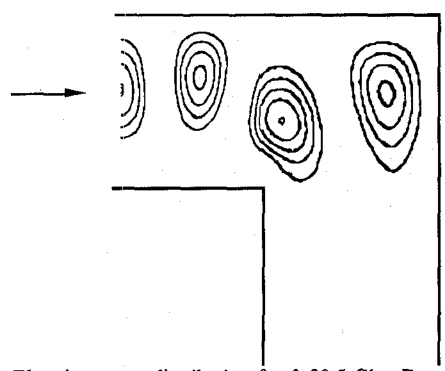

Figure 11. Electric energy distribution for f=39.5 Ghz. $E_{max}=2.21\cdot10^{-7}$ J/m^3.

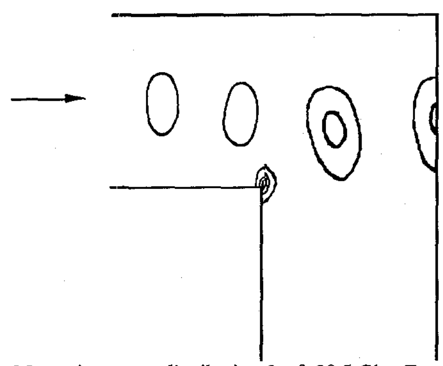

Figure 12. Magnetic energy distribution for f=39.5 Ghz. $E_{max}=4.65\cdot10^{-7}$ J/m^3.

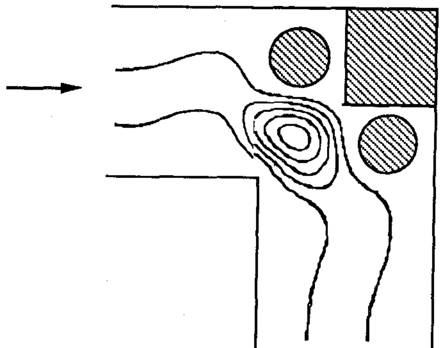

Figure 13. Electric energy distribution of the matched configuration for f=38 Ghz. $E_{max}=1.32 \cdot 10^{-7}$ J/m^3.

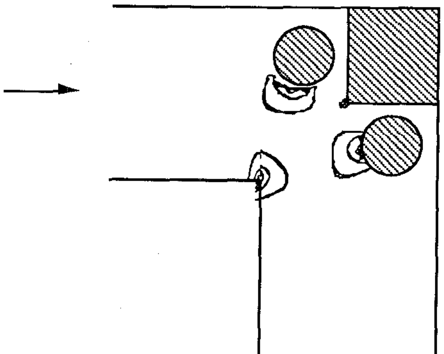

Figure 14. Magnetic energy distribution of the matched configuration for f=38 Ghz. $E_{max}=2.64 \cdot 10^{-7}$ J/m^3.

valid few millimeters away from the corner where cut off modes are negligible). Figures 11 and 12 show the electrical and magnetic energies for the same corner at frequencies of 39.5 GHz respectively. It is noted how the fields do not propagate beyond the corner. Figure 13 shows the electrical energy for the matched configuration at the frequency of 38 GHz, while figure 14 shows the magnetic energy at the same frequency. It is also noted how the fields propagate beyond the corner.

CONCLUSIONS

This work demonstrates the derivation of wideband equivalent circuits from the FD-TD analysis and their subsequent use in practical CAD and synthesis situations. The inductive post and the 90° H-plane corner are taken as specific examples. Circuit models of the two discontinuities are derived. Full band matching of the undercut corner by means of two small inductive posts is obtained. Theoretical predictions and experimental results are in excellent agreement while a reflection lower than -12 dB over the wide K_A-band is achieved for the matched configuration.

ACKNOWLEDGEMENT

William Gullock of Alcaltel-Telettra, Antonio Morini and Andrea Schiavoni of University of Ancona are gratefully acknowledged for helpful discussion.

REFERENCES

[1] K.S. Yee, "Numerical Solutions of Initial Boundary Value Problems Involving Maxwell's Equation in Isotropic Media," *IEEE Trans. on Antennas Propagation,* vol. AP-14, pp. 302-307, 1966.

[2] G. Mur, "Absorbing Boundary Conditions for the Finite-Difference Approximation of the Time Domain Electromagnetic Field Equations," *IEEE Trans. Elect. Comp.*, vol. EMC-23, pp. 377-382, 1981.

[3] G. Mur, "The Modelling of Singularities in the Finite-Difference Approximation of the Time-Domain Electromagnetic-Field Equations," *IEEE Transactions on Microwave Theory and Techniques*, vol. MTT-29, pp. 1073-1077, 1981.

[4] F. Moglie, T. Rozzi, P. Marcozzi, A. Schiavoni, "A New Termination Condition for the Application of FD-TD Techniques to Discontinuity Problems in Close Homogeneous Waveguide," *IEEE Microwave and Guided Wave Letters*, pp 475-477, 1992.

[5] T. Rozzi, F. Moglie, A. Morini, W. Gulloch, and M. Politi, "Accurate Full-Band Equivalent Circuits of Inductive Posts in Rectangular Waveguide," *IEEE Transactions on Microwave Theory and Techniques*, vol. MTT-40, pp. 1000-1009, 1992.

[6] N. Marcuvitz, "Waveguide Handbook", Mc Graw Hill.